Cytoplasmic eIF6 Promotes OSCC Malignant Behavior Through AKT Pathway

Zechen Zhao
Nanjing Medical University
Weming Chu
Nanjing Medical University
Yang Zheng
Nanjing Medical University
Chao Wang
Nanjing Medical University
Yuemei Yang
Nanjing Medical University
Teng Xu
Nanjing Medical University
Xueming Yang
Nanjing Medical University
Wei Zhang
Nanjing Medical University
Xu Ding
Nanjing Medical University
Gang Li
Xuzhou Medical University
Hongchuang Zhang
Xuzhou No.1 Peoples Hospital
Junbo Zhou
Nanjing Integrated Traditional Chinese and Western Medicine Hospital
Jinhai Ye
Nanjing Medical University
Heming Wu
Nanjing Medical University
Xiaomeng Song
Nanjing Medical University
Yunong Wu (yunongwu@njmu.edu.cn)
Nanjing Medical University https://orcid.org/0000-0001-9863-7840

Research article

Keywords: OSCC, eIF6, EMT, AKT, cell invasion and migration

Posted Date: August 31st, 2021

DOI: https://doi.org/10.21203/rs.3.rs-845810/v1

Abstract

Background: Eukaryotic translation initiation factor 6 (eIF6), also known as integrin β4 binding protein, is involved in the formation and translation of ribosomes and acts as an anti-association factor. It is also essential for the growth and reproduction of cells, including tumor cells. Yet, its role in oral squamous cell carcinoma (OSCC) remains unclear.

Methods: The expression characteristics of eIF6 in 233 samples were comprehensively analyzed by immumohistochemical staining (IHC). Effects of eIF6 over-expression and knockdown on cell proliferation, migration and invasion were determined by CCK-8, wound healing and Transwell assays. Western blot, immunofluorescence (IF) and co-immunoprecipitation (co-IP) were performed for mechanism verification.

Results: We found that cytoplasmic eIF6 was abnormally highly expressed in OSCC tissues, and its expression was associated with tumor size and the clinical grade. Amplification of eIF6 promoted the growth, migration, and invasion capabilities of OSCC cell lines *in vitro* and tumor growth *in vivo*. Through Western blot analysis, we further discovered that eIF6 significantly promotes epithelial-mesenchymal transformation (EMT) in OSCC cells, while depletion of eIF6 can reverse this process. Mechanistically, eIF6 promotes tumor progression by activating the AKT signaling pathway. By performing co-immunoprecipitation, we discovered a direct interaction between endogenous eIF6 and AKT protein in the cytoplasm.

Conclusions: This was the first report on the role and mechanism of eIF6 in OSCC. These results demonstrated that eIF6 could be a new therapeutic target in OSCC, thus providing a new basis for the prognosis of OSCC patients in the future.

Background

Head and neck cancer is the 6th most common cancer worldwide (1), causing nearly 700,000 new cases and 380,000 deaths every year (2). The majority of these patients are diagnosed with head and neck squamous cell carcinoma, including oral squamous cell carcinoma (OSCC) (3). Despite advances in surgery, radiotherapy, and chemotherapy, 40-60% of OSCC patients have local recurrence or distant metastasis (4). Local bones and lymph nodes are common sites of metastasis, which leads to a poor prognosis and low quality of life for OSCC patients (5). To date, for locally advanced OSCC, the in-depth study of risk factors and molecular biomarkers has provided a new idea for subsequent treatment (6).

It is well known that ribosomes translate biological proteins, and the initial stage of this process is a pivotal step to regulate and limit translation (7). The eukaryotic translation initiation factors have an indispensable role at this stage, such as eIF1, eIF3, eIF5, etc. (8). eIF6, also known as integrin β4 binding protein, is mainly located in the cytoplasm of mammalian cells and partly in the nucleus. However, eIF6 is also located in individual cells' nucleolus, like HeLa, A431, Colon adenoma, and cancer cell lines (9). eIF6 can prevent the premature combination of the 40s ribosomal subunit and the 60s ribosomal subunit in

the translation initiation stage, thus exerting its role in rate-limiting regulation (10). eIF6 has a unique effect on the regulation of biological growth and development (11). In Xenopus, over-expressing eIF6 can lead to delayed eye development (12). Gipc2 regulated by eIF6 can ensure the Xenopus eye's normal morphology development and stimulate the relative molecular network, such as the AKT signaling pathway (13). In mammals, eIF6 acts on adipogenic transcription factors, such as C/EBPb, C/EBPd, and ATF4, thereby affecting lipid metabolism and glycolysis level (14). Given the powerful translation control capabilities of eIF6, we began to explore whether it continues to be important in cancer development.

According to previous studies, eIF6 is abnormally expressed in human cancer tissues (9). In thyroid carcinoma, eIF6 promotes tumor growth by regulating MIR-144-3p/TGF-α, and knockout of eIF6 enhances cisplatin sensitivity (15). In non-small cell lung cancer, the expression of eIF6 is higher than in normal tissues. Knocking out eIF6 leads to pre-rRNA processing and 60s ribosome maturation defects (16). In addition, eIF6 is related to patients' survival rate in colorectal cancer. Its absence can inhibit cell proliferation and invasion (17). Besides, studies have suggested that eIF6 in tumors is related to its hyperphosphorylation (18). When eIF6 takes effect, it remarkably upregulates the functional network related to cell movement, like the CDC22, which can significantly increase the migration and invasion of tumor cells (19).

During embryonic development, cell epithelium's transition to mesenchymal state is a highly plastic and dynamic process called epithelial-mesenchymal transition (EMT) that allows migration and invasion behavior (20). In malignant cells, EMT transcription factors, such as ZEB1(Zinc-finger E-box binding homeobox 1) and ZEB2 (Zinc finger E-box binding homeobox 2) can lead to E-cadherin transcriptional repression and a rise in N-cadherin and vimentin (21, 22). According to reports, p-ERK-eIF2α (protein kinase RNA-like ER kinase-eIF2) is signal transduction necessary to maintain endoplasmic reticulum homeostasis, which is also important for the invasion of EMT cells (23). EIF5A2 promotes the invasion and metastasis of liver cancer by inducing EMT and activated RhoA and Rac1 (Rho-family small GTPases) to cause cytoskeletal rearrangement (24). However, whether eIF6 can affect the full migration and invasion capabilities of OSCC remains unclear.

In this study, we found that cytoplasmic eIF6 might have a vital role in the progression of OSCC and mediate AKT-related signaling pathways. In OSCC, a high expression of eIF6 activated EMT to promote cell migration and invasion. On the other hand, the knockdown of eIF6 reversed this process. AKT pathway inhibitor, LY294002, reversed the oncogenic phenotype of eIF6 in OSCC. By performing Co-IP, we discovered a physical binding between endogenous eIF6 and AKT protein. This was the first time that we discovered a tumorigenic role of cytoplasmic eIF6 in OSCC. Exploring the deep mechanism of eIF6 may provide us with new molecular targeting treatment ideas.

Materials And Methods

Patients and Tissue Samples

Tumor microarrays were assessed in this study. A total of 233 patient samples were collected from the Stomatological Hospital of Jiangsu Province (In 2014-2019), including 206 primary OSCC samples and 27 normal oral mucosae. Clinical and pathological data were listed in **Table 1**. Patient clinical information included age, gender, location, tumor size, histological grade, metastatic lymph node, clinical stage (defined by the American Joint Committee on Cancer 7th edition), and postoperative survival rate (as of April 2021). Besides, we collected 8 samples of tumor tissues and adjacent normal tissues from patients diagnosed with OSCC from the Stomatological Hospital of Jiangsu Province (In 2020). Moreover, all samples were stored in -80℃ liquid nitrogen for subsequent experiments. Corresponding clinicopathological data are shown in Table S1.

This study was approved by the Ethics Committee of Nanjing Medical University. Informed consent was obtained from all patients.

Immunohistochemistry

Tissue microarrays were stained with primary antibodies against eIF6 (diluted 1:200, Abcam) overnight following secondary antibody incubation for 30 minutes. All of the sections were counterstained using haematoxylin, dehydrated, cleared and mounted before examination using a microscope (DM4000B, Leica, Germany). eIF6 immunoreactivity in microarray samples was calculated according to staining concentration and proportion semi-quantitatively. The score for the scale of positive cells was demonstrated as follows: 0, negative; 1, < 20%; 2, 20- 50%; 3, 51-75%; and 4, > 75% positive cells. For staining strength, grading system was classified as below: 0, no staining; 1, light yellow; 2, brownish yellow; 3, dark brownish yellow. The result was calculated by multiplying the two scores as mentioned above. Scores for > 4 points were regarded as positive.

Cell culture and inhibitor

Human OSCC cell lines HN4 and HN6 were obtained from the Shanghai Ninth People's Hospital (Shanghai, China). Cells were cultured in Dulbecco's Modified Eagle Medium (DMEM) containing 10% FBS (FBS, HyClone, USA) in a humid environment at 37°C with 5% CO□. LY294002 was purchased from Selleck (Selleck Chem, Houston, USA) and was dissolved in Dimethyl Sulphoxide (DMSO). DMSO was used for control.

Cell transfection

eIF6, negative control (NC), sh-NC and sh-eIF6 (sh-eIF6-1, sh-eIF6-2) were all purchased from GemmaPharma (Suzhou,China). According to the manufacturer's protocol, plasmids were transfected into HN4 and HN6 cells using Lipofectamine 2000 (Invitrogen, Carlsbad, USA). The transfected cells were cultured in a complete medium for at least 48 hours before performing the next experiment.

Western blot

Total protein was lysed with lysis buffer (Beyotime, China) containing phosphatase inhibitor and protease inhibitor cocktails. Utilizing Coomassie Brilliant Blue as the standard, protein lysate was quantified with the bovine serum albumin (BSA). The total proteins were loaded into SDS-polyacrylamide gels and then transferred to polyvinylidene difluoride (PVDF) membranes (Millipore) with 5% BSA at room temperature for 2h. Next, the membrane was incubated with primary antibodies (diluted 1:1000) specific for eIF6 (Abcam), E-cadherin, Vimentin, N-cadherin, AKT, p-AKT, and PI3K (CST), EGFR, p-EGFR, and β-actin (Bioworld, China), ZEB1 and ZEB2 (Proteintech, USA) and incubated overnight at 4℃. Samples were then washed three times with PBST for 10 minutes and incubated with anti-goat IgG HRP-conjugated secondary antibodies (Zhongshan Goldenbridge Bio, China) for 1 hour at room temperature. Finally, the immunoreactive bands were detected by Immobilon Western Chemiluminescent HRP Substrate (Millipore) and visualized with the ImageQuantLAS4000 mini imaging system (General Electric). ImageJ software was used for gray value analysis and β-actin was used as an internal control. Each experiment was independently repeated three times and quantitatively analyzed.

RNA extraction and quantitative reverse transcription PCR (qRT-PCR)

According to the reagent instructions, total RNA was obtained using TRIzol reagent (Invitrogen) and then reverted to cDNA using 5 × PrimeScript RT Master Mix (TaKaRa) after 15 minutes at 37℃ and 5 seconds at 85℃. Quantitative Real-Time PCR in a 7900HT Real-Time PCR System (Applied Biosystems). The RNA levels of eIF6 and GAPDH were determined with the following primers: eIF6: F: 5'-CCGACCAGGTGCTAGTAGGAA-3', R: 5'- CAGAAGGCACACCAGTCATTC-3'; AKT: F: 5'-AGCGACGTGGCTATTGTGAAG-3', R: 5'- GCCATCATTCTTGAGGAGGAAGT-3'; EGFR:F: 5'-AAAGTTAAAATTCCCGTCATCAG-3', R: 5'-TCACGTA GGCTTCATCGAGATTTC-3' ; PIK3CA:F: 5'-CCACGACCATCATCAGGTGAA-3', R: 5'- CCTCACGGAGGCATTCTAAAGT-3'; PIK3CB: F: 5'-TATTTGGACTTTGCGACAAGACT-3', R: 5'- TCGAACGTACTGGTCTGGATAG-3'; GAPDH: F: 5'-GAAGGTGAAGGTCGGAGT C-3', R: 5'- GAGATGGTGATGGGATTTC –3'. The result was quantified by the delta-delta Ct method to quantify the relative gene expression. The average expression of each gene was normalized to the geometric mean of GAPDH.

Cell viability and colony formation assay

For cell viability experiment, cells were seeded in a 96-well plate at a density of 2000 cells per well and cultured at 37℃ for 0-7 days. After each time point, 10% CCK-8 reaction solution (DOJINDO, Japan) was added to each well and incubated for another 2 h at 37°C medium to culture the cells to be measured for 2 hours. The absorbance was quantified on a spectrophotometer microplate reader (Multiskan MK3, Thermo) with 450 nm wavelength. Eight experiments were independently conducted every day.

For the colony formation experiment, cells were cultured in 60-mm dish (Corning) with 2000 cells per dish for 14 days. Cells were then fixed with 4% paraformaldehyde (PFA), stained with crystal violet, and analyzed by microscopy.

Transwell assay

Cell invasion ability was analyzed through Transwell filters (8 mm pore size; Millipore) coated with 50 mL Matrigel Basement Membrane Matrix (BD Biosciences). The cells (40000 cells) were seeded in the upper chamber containing 200μL of serum-free medium, while 800μL of 10% serum medium was placed in the lower chamber. After indicated time point, cells in the upper chamber were fixed with 4% PFA for 30 minutes, stained with crystal violet, and analyzed under the microscope (ZEISS, Germany).

Wound healing assays

The cell migration was performed using a wound-healing assay. Briefly, cells were seeded in a 6-well plate at 2000 cells per well for 24 hours. A line was then drawn using a marker on the bottom of the dish, after which a sterile 10μL pipet tip was used to scratch three separate wounds through the cells, moving perpendicular to the line. The cells were gently rinsed twice with PBS to remove floating cells and incubated in cultured in a serum-free medium. Images of the scratches were taken by using an optical microscope (Leica, Germany) at ×10 magnification at indicated time of incubation, and the healing area was analyzed with ImageJ software (Wayne Rasband National Institutes of Health, USA).

Immunofluorescence staining

HN6 transfected cells were cultured on the sterile glass-coverslips in 24-well plates for 12 hours. Cells were then fixed with 4% PFA and permeabilized with 1% Triton and blocked with goat serum for 30 minutes. In the shaded condition, the cells were incubated with the eIF6 (diluted 1:100, Abcam) or AKT (diluted 1:100, CST) or p-AKT (diluted 1:200, CST) antibodies at 4℃ overnight and then stained with goat anti-rabbit IgG antibody Cy3 (Proteintech, China) for 1 hour at 37℃. After staining with DAPI (Sigma, St Louis, MO), cells were analyzed using fluorescence microscopy (ZEISS, Germany).

Subcutaneous tumor model

Twenty male BALB/c athymic nude mice (five-week-old) were purchased from the Animal Core Facility of Nanjing Medical University (Nanjing, China). All the animals were housed in an environment with a temperature of 22 ± 1 ºC, relative humidity of 50 ± 1%, and a light/dark cycle of 12/12 hr. All animal studies (including the mice euthanasia procedure) were done in compliance with the regulations and guidelines of Nanjing Medical institutional animal care and conducted according to the AAALAC and the IACUC guidelines.

Animals were randomly divided into 4 groups (5 mice per group): NC, eIF6, sh-NC, and sh-eIF6. Stably transfected HN6 cells resuspended in 50% matrigel were subcutaneously injected into the nude mice flank (1×10^7 cells/100 μL). The xenograft tumor size was checked every three days and measured with a vernier caliper. The formula that was used to measure the tumor volume was: *[volume = (length × width²)/2]*. Twenty days after the injection, the nude mice were executed, and the tumor tissues were dissected out, imaged, and weighed up.

Statistical Analysis

Statistical analysis is processed using graphing software GraphPad Prism version 8.0.1 (Graph Pad Software Inc., La Jolla, CA, USA). All experiments are repeated at least 3 times. The data index of each experiment represents the mean ± SD from 3 independent experiments. Use the Student's t-test to calculate the statistical significance of experimental data. All P values represent statistically significant two-sided tests (*P < 0.05, **P < 0.01, ***P < 0.001).

Results

Cytoplasmic eIF6 is overexpressed in OSCC and is associated with poor prognosis

To explore how eif6 is expressed and whether it has a role in OSCC, we conducted differential expression analysis in the TCGA database by an interactive web portal, UALCAN (http://ualcan.path.uab.edu) (25). The results showed a marked difference in eIF6 expression between the tumor and non-tumor groups, and the difference was statistically significant (**Figure 1A**). Then we performed a tissue microarray analysis, including 206 tumor tissues and 27 non-tumor tissues. Among 206 tissues, 22 tissues showed a nucleus expression of eIF6. In 25 tumor tissues, eIF6 was expressed in both nucleus and cytoplasm. Cytoplasmic-specific expressing eIF6 was observed in 184 tissue sections, which were further analyzed by clinicopathological features (**Table 1**). In normal oral mucosa, eIF6 was mostly confined to the nucleus with lower expression compared with tumor tissues (**Figure 1B** and **1E**). We also found that low expression of nucleus eIF6 was associated with poor prognosis, indicating the positive role of the nucleus eIF6 in OSCC (**Figure 1C**). However, there was no prognostic difference in the nucleus and cytoplasmic co-expression of EIF6 between the low- and high-expression group (**Figure 1D**). Notably, in tumor tissues, eIF6 was mostly diffused in the cytoplasm (**Figure 1E**). High cytoplasmic eIF6 staining was significantly associated with advanced tumor size, lymph node metastasis, and clinical stage (**Figure 1F** and **Table 1**). No significant difference was shown in the pathological stage. The Kaplan-Meier curves indicated that increased cytoplasmic eIF6 expression was related to lower overall survival in OSCC patients (**Figure 1G**).

We then collected 8 OSCC tumor tissues and the same amount of normal tissues from the clinic. Through Western blot (n=6) and qRT-PCR (n=8) analysis, we found that eIF6 was overexpressed in OSCC than in normal tissues (**Figure 1H-I**). These results indicated that the presence of eIF6 has an essential role in OSCC.

eIF6 enhances OSCC proliferation *in vitro and in vivo*

In order to determine the function of eIF6 in tumor progression, we performed gain-of-function or loss-of-function assays in HN4 and HN6 OSCC cell lines. The efficiency of infection was confirmed by qRT- PCR. Marked increase or depletion of eIF6 expression level was observed in **Figure 2A**. Through the above research, we began to explore how eIF6 affects the phenotype of OSCC cells. Transfection with eIF6 formed larger colonies and improved cell proliferation ability (**Figure 2B**). Flow cytometry analysis confirmed the proliferative tendency in eIF6 over-expression group (**Figure 2C**). Moreover, the CCK8 assay of eIF6 overexpression was investigated with HN4 and HN6 cells (**Figure 2D**). The rate of cell growth and proliferation significantly increased compared with control. Furthermore, the inhibition of eIF6 formed

fewer colonies, and reduced cell proliferation (**Figure 2E-F**). CCK-8 assays confirmed the anti-proliferative effect of eIF6 in OSCC cell lines (**Figure 2G**).

Next, we analyzed the effects of eIF6 *in vivo*. The NC, eIF6, sh-NC and sh-eIF6 encoding vectors were transfected into HN6 cell lines, respectively. Then, the transformed HN6 cell lines were subcutaneously inoculated in BALB/C nude mice in 4 groups. The tumors were dissected 20 days after tumor formation. As shown in **Figure2H**, cells overexpressing eIF6 grew faster (higher tumor weight and volume) than the cells expressing eIF6 encoding vectors or control vector. By contrary, eIF6 depletion attenuated tumor formation in vivo (**Figure 2I**).

High expression of eIF6 can induce epithelial-mesenchymal transition, while knockdown of eIF6 reversed this process

To explore whether eIF6 can regulate EMT in OSCC, we stably transfected control and eIF6 encoding vectors into HN4 and HN6 cell lines. Overexpression of eIF6 significantly strengthened the invasion ability (**Figure 3A**) and cell migration compared to the control group (**Figure 3B**) in HN4 and HN6 cells. Conversely, the inhibition of eIF6 inhibited cell invasion and migration (**Figure 3C-D**). Subsequently, we studied the relationship between high expression of eIF6 and EMT in HN4 and HN6 cells. We measured the expression of EMT-related markers through Western blot analysis (**Figure 3E**). High expression of eIF6 down-regulated the epithelial markers E-cadherin and upregulated mesenchymal markers N-cadherin and Vimentin, as well as transcription factors Zeb1 and Zeb2. These results revealed that over-expression of eIF6 induced EMT in HN4 and HN6 cells. Contrary, the knockdown of eIF6 reversed this process, i.e., E-cadherin protein content increased, while N-cadherin, Vimentin, Zeb1, and Zeb2 significantly decreased (**Figure 3F**). This result showed to some extent that knocking down eIF6 can reverse the EMT phenomenon in OSCC cells.

eIF6 effect is related to the AKT signaling pathway

Previous experiments have shown that eIF6 may be related to the AKT signaling pathway (26). To further explore the relationship between eIF6 and AKT signaling pathway in OSCC cells, we first measured the cells' mRNA changes associated with the AKT signaling pathway when eIF6 was amplified. In cells overexpressing eIF6, EGFR, phosphatidylinositol 3-kinase catalytic subunit alpha (PIK3CA), PIK3CB, and AKT were slightly increased (**Figure 4A**); this process was reversed when knocking down eIF6 (**Figure 4A**). Next, we performed Western blot and found that the high expression of eIF6 had protein effects on the AKT pathway-related markers (**Figure 4B**). In HN4 and HN6 cells, the results showed that the expressions of phospho-EGFR (p-EGFR), PIK3CA, PIK3CB, and p-AKT were higher than those of the control group, but the changes of EGFR and AKT were not noticeable. Furthermore, the inhibition of eIF6 in both HN4 and HN6 cells caused a visible reduction in p-EGFR, PI3K, and p-AKT protein expression (**Figure 4C**). These data indicated that the decrease in eIF6 expression could inhibit initially activated AKT pathway. To prove that cells overexpressing eIF6 do activate AKT signaling, we inhibited the AKT signaling pathway. LY294002, a PI3K inhibitor, was used in HN4 and HN6 cell lines overexpressing eIF6. Notably, LY294002 decreased the oncogenic phenotype of eIF6 by depressing proliferative, invasive and migrative ability

(**Figure 4D-F**). Furthermore, LY294002 significantly down-regulated the protein expression of PI3K and p-AKT in the cells transfected with eIF6 (**Figure 4G**), suggesting a crosstalk between eIF6 and PI3K-AKT pathway.

eIF6 participates in the activation of AKT in the cytoplasm

In our previous study, we have discovered the oncogenic role of cytoplasmic eIF6 in tumor tissues by microarray analysis (**Figure 1G**). We then investigated the physical localization of eIF6 in OSCC cells. Confocal microscopy showed that eIF6 was mainly expressed in the cytoplasm upon eIF6 amplification compared with control cells where eIF6 was demonstrated in the nucleus (**Figure 5A**). AKT and p-AKT expression levels were then examined by immunofluorescence. Over-expression of eIF6 resulted in an activation of AKT pathway with an increased immunostaining of AKT and p-AKT in the cytoplasm (**Figure 5B-C**). Decreased nuclear translocation of AKT and increased phosphorylation of AKT were detected in eIF6-over-expressing cells; however, cells in the control group exhibited the opposite pattern of nuclear translocation and phosphorylation. Protein separation techniques were utilized to determine the protein level of subcellular fractions. Western blotting was performed to assess the expression of eIF6 and AKT pathway proteins in cytoplasmic and nuclear extracts from eIF6-over-expressed or control cells. Cytoplasmic expression of eIF6, AKT and p-AKT in eIF6-over-expression group was increased compared with control (**Figure 5D**). Meanwhile, eIF6 inhibition displayed an opposite effect (data not shown). We then analyzed cell-cycle related proteins by performing Western blotting. We found that amplification of eIF6 resulted in an up-regulation of cytoplasmic CDK (CDK2, 4) and cyclin (cyclin D1, cyclin D3 and cyclin E1) proteins in both HN4 and HN6 cell lines (**Figure 5E**). These results suggested that functional eIF6 was retained in the cytoplasm and regulated cell-cycle checkpoints by activating AKT pathway.

eIF6 physically interacts with AKT

To further determine whether there was a direct interaction between endogenous eIF6 and AKT protein, we investigated the protein-protein interaction by immunoprecipitation assay in OSCC cells (**Figure 6A**). Endogenous eIF6 was co-immunoprecipitated with endogenous AKT in the cytoplasm in both HN4 and HN6 cells. Cells were then treated with MG132 (10 μM) for the indicated times, and then the levels of eIF6 and AKT were detected. MG132 enhanced both eIF6 and AKT protein levels in a time-dependent manner (**Figure 6B**). Opposite effect was observed in CHX-treated OSCC cells (**Figure 6C**). Then cells over-expressing eIF6 were treated with or without MG132, and the eIF6 and AKT protein levels were assessed by Western blotting (**Figure 6D**). Ectopic expression of eIF6 increased the amount of AKT when exposed to MG132. CHX treatment resulted in adverse impact (**Figure 6E**). Furthermore, with the exposure of MG132, ectopic expression of eIF6 increased the amount of co-immunoprecipitated AKT (**Figure 6F**). These data indicated that cytoplasmic eIF6 mediated the AKT binding, thereby facilitating AKT pathway activation.

Discussion

eIF6 is the primary regulator of translation and tumor progression *in vivo*. In the cytoplasm, it affects the assembly of 80S by binding to 60S ribosomes (27). eIF6 is also believed to be a cancer-related biomarker and a potential therapeutic target for malignant tumors (28). Changes in eIF6 have been found in some malignant tumors. Its high expression was found in HNSCC (29). In this study, we investigated the regulation of eIF6 on OSCC and its possible mechanism. We performed a microarray analysis of tumor tissue samples from 206 patients and noticed that eIF6 was highly expressed in cancer tissues compared to normal tissue. Moreover, cytoplasmic eIF6 was significantly correlated with the tumor size, lymph node metastasis and clinical stage of patients. We also observed that high expression of cytoplasmic eIF6 indicated a poor prognosis in the survival curve. These results suggested that eIF6 could be a diagnostic and prognostic marker for OSCC.

Here, we used plasmids over-expressing or depleting of eIF6 to examine its role in OSCC. Results showed that high expression of eIF6 could increase the biological behavior of OSCC, including cell viability, proliferation, invasion, and migration. Knockdown of eIF6 can significantly inhibit this cancer-promoting effect. Thus, we hypothesized that it is the abnormal accumulation of eIF6 in cells that leads to the continuous deepening of the malignancy of OSCC.

Generally, the aggressiveness and metastasis of OSCC are the main reasons for the poor prognosis (30). In order to develop metastasis, tumor cells need to acquire aggressive activity. Epithelial-mesenchymal transition (EMT) can induce cells to change their morphology, lose their polarity, and increase invasiveness. Therefore, it is easier for tumor cells to transfer from the original environment to distant places (31). Translation factors, such as the p-ERK/eIF2/ATF4 signaling pathway, have been involved in EMT in pancreatic cancer cells (32). In this study, eIF6 overexpression decreased E-cadherin expression levels and increased N-cadherin, Vimentin, ZEB1, and ZEB2, thus suggesting that the eIF6 upregulation promotes EMT in OSCC. We assumed that eIF6 may be a key driver of EMT. After knocking out eIF6, a significant reversal of EMT can be observed. Similarly, the initially high invasion and migration capabilities of OSCC cells were also suppressed. Thus, we predicted that eIF6 regulates OSCC cell migration and invasion by activating EMT.

The initial stage is often regarded as the rate-limiting step of translation (10). Translation disorders are ubiquitous in human cancers. Numerous reports have confirmed that targeting translation mechanisms in tumors is practical and feasible (33). For instance, mRNA binding to ribosomes in eukaryotes is based on the eIF4 factor, which is composed of the eIF4F complex and eIF4B. After binding to the eIF4 factor, activated mRNA is recruited by the 43S pre-initiation complex (PIC). Then, the mRNA 5' end combines with 43S PIC to form 48S PIC (34). Significantly, the formation of 48S PIC is obviously affected by mTOR complex 1 (mTORC1), which promotes the phosphorylation of eIF4E binding protein and allows the eIF4F complex to be produced. Based on this mechanism, mTORC1 inhibitors have been developed for clinical studies. However, problems cannot be ignored, such as long-term exposure to mTORC1 specific inhibitors that can promote drug resistance and/or activate other AKT-regulated pathways (35). These problems may significantly reduce his original efficacy. Thus, new directions are urgently needed to make up for such drugs' shortcomings.

Epidermal growth factor receptor (EGFR) belongs to the receptor tyrosine kinases, which is highly expressed in most OSCC and is associated with poor prognosis (36). The EGFR/phosphoinositide 3-kinase (PI3K)/AKT pathway has an important role in cell physiology, activating mTOR to participate in a wide range of life activities, including proliferation, growth, movement, and metabolism. It responds to extracellular stimuli and triggers a variety of signal transductions (37). Due to the frequent observation of mutations in this pathway in cancer, drugs targeting PI3K, AKT, and mTOR are under active development (38). Over recent years, studies have suggested that the translation behavior of eIF6 is not regulated downstream of the mTOR signaling pathway. Specifically, the activation of eIF6 is derived from phosphorylation caused by the protein kinase C system (PKC), not mTORC1(39). This means that regulating eIF6 may effectively avoid the emergence of mTOR-resistance, and the new target may bring better efficacy for clinical treatment. Nonetheless, the mechanism underlying eIF6 action is still not clear.

Interestingly, it is reported that eIF6 can actively regulate AKT-related cancer signaling and enhance the tumorigenicity of colorectal cancer (26). Some scholars have found significantly enriched eIF6 expression and PI3K/AKT/mTOR signals in colorectal adenomas (40). As the classical upstream regulator of AKT, EGFR also has a regulatory connection with the eukaryotic translation factor (41). Our study suggested that eIF6 amplification could increase p-EGFR, PI3K, and p-AKT, but not EGFR and AKT. At the same time, knocking down eIF6 showed an inhibitory effect on the corresponding indicators. These results suggested that eIF6 can stimulate the PI3K/AKT cascade, which is consistent with the tumor cell phenotype after eIF6 amplification. Crucially, the PI3K/AKT signaling pathway may also have an essential role in eIF6-mediated EMT.

To confirm that eIF6 is indeed involved in the PI3K/AKT cascade reaction, LY294002, an inhibitor of PI3K, was used to further process the cells. It has been clinically proven that LY294002 has significant effects on inhibiting tumor growth and treatment (42). In theory, if eIF6 is involved in the PI3K/AKT cascade, then PI3K inhibition may prevent this process. From the experimental results, the AKT pathway was originally activated by PI3K, and a significant inhibitory effect occurred after LY294002 treatment, which could be observed in both cell lines overexpressed eIF6. We did not observe complete inhibition of p-AKT, which suggested that there may still be other ways to activate the AKT pathway. But this also confirms that even with higher eIF6 levels, PI3K inhibition can still directly block AKT regulated by eIF6. Mechanically, we found that eIF6 could directly bind with AKT in the cytoplasm, indicating the physical interaction between two proteins. We also found that after eIF6 was amplified, the subcellular localization of eIF6 was significantly changed. It appeared in large numbers in the cytoplasm but rarely accumulated in the nucleus. This indicated that accelerating the nuclear transport of eIF6 may be closely related to the invasion and metastasis of cancer. However, further experiments are needed to explore what processes eIF6 goes through in the nucleus, whether its release from the nucleus is regulated in some way, and whether eIF6 in the cytoplasm is an inducing factor.

Conclusion

This was the first report on the role and mechanism of eIF6 in OSCC (Fig. 6G). Our study explained the underlying mechanism of eIF6-related phenotypes and emphasized the critical part of the AKT signaling pathway in eIF6-mediated cancer. In the clinic, eIF6 is expected to become an essential criterion for diagnosing the tumor condition and judging the prognosis. It also provides a new direction for future research on the role of eIF6 in tumor progression and drug resistance.

Abbreviations

OSCC: oral squamous cell carcinoma; eIF6: Eukaryotic translation initiation factor 6;IHC: immumohistochemical staining; IF: immunofluorescence; co-IP: co-immunoprecipitation; EMT: epithelial-mesenchymal transformation; ZEB1: Zinc-finger E-box binding homeobox 1; ZEB2: Zinc finger E-box binding homeobox 2) ; p-ERK-eIF2α: protein kinase RNA-like ER kinase-eIF2; Rac1: Rho-family small GTPases; PIK3CA: phosphatidylinositol 3-kinase catalytic subunit alpha; mTORC1: mTOR complex 1; EGFR: Epidermal growth factor receptor; PKC: protein kinase C system

Declarations

Acknowledgements

None.

Authors' Contributions

Z.C. Zhao, W.M. Chu, Y. Zheng and Y.N. Wu designed the study and wrote the manuscript; C. Wang, Y.M. Yang and T. Xu performed cellular experiments and analyzed the data; X.M. Yang, W. Zhang and X. Ding performed RT-PCR and the study of the signaling pathway; J.B. Zhou participated in bioinformatic analysis; G. Li and H.C. Zhang helped conduct the migration and invasion assay; J.H. Ye, H.M. Wu and X.M. Song helped some animal experiments and revised the manuscript. All of the authors reviewed the manuscript before submission and approved the final manuscript.

Funding

This research was supported by the National Natural Science Foundation of China (81402236, 81772887), the Priority Academic Program Development of Jiangsu Higher Education Institutions (PAPD, 2018-87), Jiangsu Provincial Medical Innovation Team (CXTDA2017036), Natural Science Foundation of Jiangsu Province of China (BK20171488) and Jiangsu Provincial Medical Youth Talent (QNRC2016854). The authors declare that they have no conflict of interest.

Availability of data and materials

All data generated or analyzed during this study are included in this published article.

Ethics approval and consent to participate

All the protocols involved in our experiments were approved by the Ethics Committee of Nanjing Medical University and study methodologies conformed to the standards set by the Declaration of Helsinki.

Consent for publication

Not applicable.

Competing Interests

The authors declare no potential conflicts of interest.

References

1. Zibelman M, Mehra R. Overview of Current Treatment Options and Investigational Targeted Therapies for Locally Advanced Squamous Cell Carcinoma of the Head and Neck. Am J Clin Oncol. 2016;39:396–406.
2. Cohen EEW,, et al. The Society for Immunotherapy of Cancer consensus statement on immunotherapy for the treatment of squamous cell carcinoma of the head and neck (HNSCC). J Immunother Cancer. 2019;7:184.
3. Johnson DE,, et al. Head and neck squamous cell carcinoma. Nat Rev Dis Primers. 2020;6:92.
4. William WN Jr., *et al.*. Erlotinib and the Risk of Oral Cancer: The Erlotinib Prevention of Oral Cancer (EPOC) Randomized Clinical Trial. JAMA Oncol. 2016;2:209–16.
5. Cheung LC, et al. Risk-Based Selection of Individuals for Oral Cancer Screening. J Clin Oncol. 2021;39:663–74.
6. Anderson CM,, et al. Phase IIb, Randomized, Double-Blind Trial of GC4419 Versus Placebo to Reduce Severe Oral Mucositis Due to Concurrent Radiotherapy and Cisplatin For Head and Neck Cancer. J Clin Oncol. 2019;37:3256–65.
7. Aylett CH, Ban N. (2017) Eukaryotic aspects of translation initiation brought into focus. *Philos Trans R Soc Lond B Biol Sci* 372.
8. Voigts-Hoffmann F, Klinge S, Ban N. Structural insights into eukaryotic ribosomes and the initiation of translation. Curr Opin Struct Biol. 2012;22:768–77.
9. Zhu W, Li GX, Chen HL, Liu XY. The role of eukaryotic translation initiation factor 6 in tumors. Oncol Lett. 2017;14:3–9.
10. Miluzio A, Beugnet A, Volta V, Biffo S. Eukaryotic initiation factor 6 mediates a continuum between 60S ribosome biogenesis and translation. EMBO Rep. 2009;10:459–65.
11. Russo A, et al. Modulating eIF6 levels unveils the role of translation in ecdysone biosynthesis during Drosophila development. Dev Biol. 2019;455:100–11.
12. De Marco N, Tussellino M, Vitale A, Campanella C. Eukaryotic initiation factor 6 (eif6) overexpression affects eye development in Xenopus laevis. Differentiation. 2011;82:108–15.

13. De Marco N, et al. Eukaryotic initiation factor eIF6 modulates the expression of Kermit 2/XGIPC in IGF- regulated eye development. Dev Biol. 2017;427:148–54.
14. Brina D, et al. eIF6 coordinates insulin sensitivity and lipid metabolism by coupling translation to transcription. Nat Commun. 2015;6:8261.
15. Liu F, et al. Circular RNA EIF6 (Hsa_circ_0060060) sponges miR-144-3p to promote the cisplatin-resistance of human thyroid carcinoma cells by autophagy regulation. Aging. 2018;10:3806–20.
16. Gantenbein N, et al. Influence of eukaryotic translation initiation factor 6 on non-small cell lung cancer development and progression. Eur J Cancer. 2018;101:165–80.
17. Golob-Schwarzl N, et al. Separation of low and high grade colon and rectum carcinoma by eukaryotic translation initiation factors 1, 5 and 6. Oncotarget. 2017;8:101224–43.
18. Miluzio A, et al. Expression and activity of eIF6 trigger malignant pleural mesothelioma growth in vivo. Oncotarget. 2015;6:37471–85.
19. Pinzaglia M, et al. EIF6 over-expression increases the motility and invasiveness of cancer cells by modulating the expression of a critical subset of membrane-bound proteins. BMC Cancer. 2015;15:131.
20. Nieto MA, Huang RY, Jackson RA, Thiery JP. Emt: 2016. Cell. 2016;166:21–45.
21. Saitoh M. Involvement of partial EMT in cancer progression. J Biochem. 2018;164:257–64.
22. Singh M, Yelle N, Venugopal C, Singh SK. EMT: Mechanisms and therapeutic implications. Pharmacol Ther. 2018;182:80–94.
23. Feng YX,, et al. Epithelial-to-mesenchymal transition activates PERK-eIF2alpha and sensitizes cells to endoplasmic reticulum stress. Cancer Discov. 2014;4:702–15.
24. Tang DJ,, et al. Overexpression of eukaryotic initiation factor 5A2 enhances cell motility and promotes tumor metastasis in hepatocellular carcinoma. Hepatology. 2010;51:1255–63.
25. Chandrashekar DS,, et al. UALCAN: A Portal for Facilitating Tumor Subgroup Gene Expression and Survival Analyses. Neoplasia. 2017;19:649–58.
26. Lin J, et al. eIF6 Promotes Colorectal Cancer Proliferation and Invasion by Regulating AKT-Related Signaling Pathways. J Biomed Nanotechnol. 2019;15:1556–67.
27. Ceci M, et al. Release of eIF6 (p27BBP) from the 60S subunit allows 80S ribosome assembly. Nature. 2003;426:579–84.
28. Brina D, Miluzio A, Ricciardi S, Biffo S. eIF6 anti-association activity is required for ribosome biogenesis, translational control and tumor progression. Biochim Biophys Acta. 2015;1849:830–5.
29. Rosso P, et al. Overexpression of p27BBP in head and neck carcinomas and their lymph node metastases. Head Neck. 2004;26:408–17.
30. Mady LJ, Nilsen ML, Johnson JT. Head and Neck Cancer in the Elderly: Frailty, Shared Decisions, and Avoidance of Low Value Care. Clin Geriatr Med. 2018;34:233–44.
31. Chen C, Zimmermann M, Tinhofer I, Kaufmann AM, Albers AE. Epithelial-to-mesenchymal transition and cancer stem(-like) cells in head and neck squamous cell carcinoma. Cancer Lett. 2013;338:47–

56.
32. Dai H, et al. PUM1 knockdown prevents tumor progression by activating the PERK/eIF2/ATF4 signaling pathway in pancreatic adenocarcinoma cells. Cell Death Dis. 2019;10:595.
33. Bhat M, et al. Targeting the translation machinery in cancer. Nat Rev Drug Discov. 2015;14:261–78.
34. Mishra RK, Datey A, Hussain T. mRNA Recruiting eIF4 Factors Involved in Protein Synthesis and Its Regulation. Biochemistry. 2020;59:34–46.
35. Barrett D, Brown VI, Grupp SA, Teachey DT. Targeting the PI3K/AKT/mTOR signaling axis in children with hematologic malignancies. Paediatr Drugs. 2012;14:299–316.
36. Pedicini P, et al. Correlation between EGFr expression and accelerated proliferation during radiotherapy of head and neck squamous cell carcinoma. Radiat Oncol. 2012;7:143.
37. Psyrri A, Seiwert TY, Jimeno A. (2013) Molecular pathways in head and neck cancer: EGFR, PI3K, and more. *Am Soc Clin Oncol Educ Book*: 246–255.
38. Guerrero-Zotano A, Mayer IA, Arteaga CL. PI3K/AKT/mTOR: role in breast cancer progression, drug resistance, and treatment. Cancer Metastasis Rev. 2016;35:515–24.
39. Miluzio A, et al. Impairment of cytoplasmic eIF6 activity restricts lymphomagenesis and tumor progression without affecting normal growth. Cancer Cell. 2011;19:765–75.
40. Komor MA,, et al. Molecular characterization of colorectal adenomas reveals POFUT1 as a candidate driver of tumor progression. Int J Cancer. 2020;146:1979–92.
41. Caraglia M, Tagliaferri P, Budillon A, Abbruzzese A. Post-translational modifications of eukaryotic initiation factor-5A (eIF-5A) as a new target for anti-cancer therapy. Adv Exp Med Biol. 1999;472:187–98.
42. Avan A, Narayan R, Giovannetti E, Peters GJ. Role of Akt signaling in resistance to DNA-targeted therapy. World J Clin Oncol. 2016;7:352–69.

Tables

Table 1. Correlation between eIF6 and clinicopathologic characteristics in 184 OSCC cases

Pathologic characteristics	n	Overexpression (number of cases)	Nonoverexpression (number of cases)	P value
Age, years				
≥ 60	98	53	45	0.1951
<60	86	46	40	
Sex				
Male	114	57	57	0.7918
Female	70	42	28	
Smoking				
Yes	76	42	34	0.2070
No	108	60	48	
Drinking				
Yes	90	49	41	0.2126
No	94	53	41	
Location				
Palate	10	4	6	0.7236
Tongue	63	33	30	
Gingiva	35	21	14	
Buccal	59	33	26	
Mouth floor	17	8	9	
Tumor stage				
T1	83	35	48	T1 vs T2 =0.0123
T2	74	46	28	T1 vs T3-4 =0.0013
T3-T4	27	21	6	
Lymph node status				
N0	99	39	60	N0 vs N1 =0.0187
N1	39	24	15	N0 vs N2-3 <0.0001
N2-3	46	35	11	
Clinical grade				

I	49	20	29	I vs II-III =0.0005
II-III	67	49	18	I vs IV <0.0001
IV	68	58	10	
Pathological grade				
I	107	58	49	I vs II =0.9052
II	58	32	26	I vs III =0.7406
III	18	9	9	

The P values represent probabilities for eIF6 expression levels between variable subgroups determined by a ^{2} test.

Figures

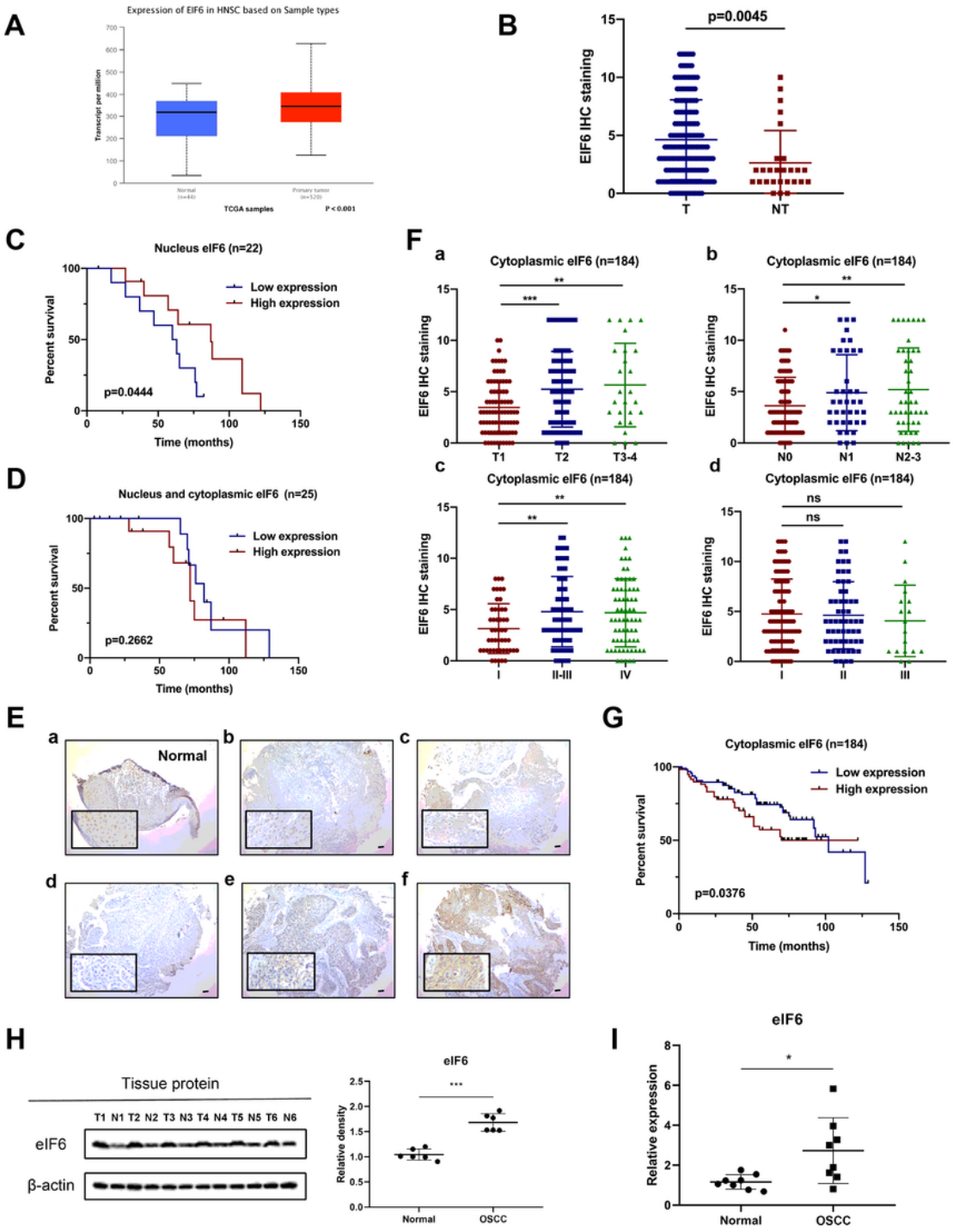

Figure 1

Cytoplasmic eIF6 is overexpressed in OSCC and is associated with poor prognosis. (A) Expression of eIF6 in HNSCC patients based on the TCGA database. (B) Pathological scores on eIF6 were assessed in tumor (T) and non-tumor (NT) tissues. (C) Low expression of nucleus eIF6 was associated with poor prognosis (n=22, p<0.005). (D) No prognostic difference was observed in the nucleus and cytoplasmic co-expression of EIF6 between the low- and high-expression group. (E) Representative IHC micrographs of

tumor microarrays sections stained with eIF6. a) non-tumor tissue; b) tumor tissue with eIF6 nucleus staining; c) tumor tissue with eIF6 nucleus and cytoplasmic co-expression; d) The weak, e) moderate and f) strong level of eIF6 staining were demonstrated. (F) The expression of eIF6 in OSCC patients with different T stage, N stage, clinical stage and pathological stage. (G)The survival curve of cytoplasmic eIF6 expression on prognosis. (H) The expression level of eIF6 protein in six tumor and adjacent non-tumor OSCC tissues. Density analysis of eIF6 signal with β-actin as the internal control. (I) The eIF6 mRNA expression in eight tumor and adjacent non-tumor OSCC tissues. In OSCC, the protein or mRNA expression of eIF6 is significantly higher than that of non-tumor tissues. All error bar values represent the SD. Scale bar, 100 μm. *P < 0.05, **P < 0.01, ***P < 0.001.

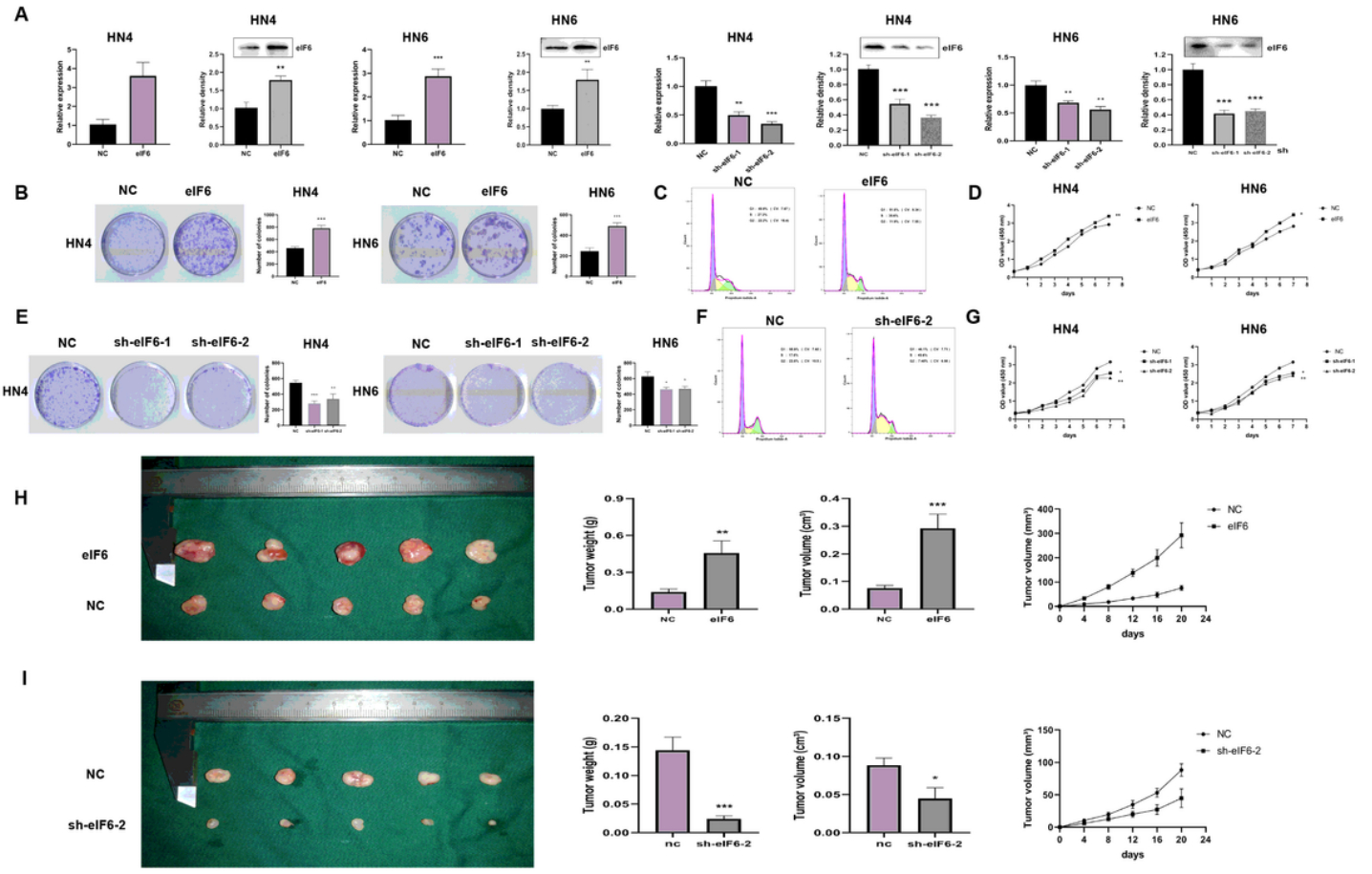

Figure 2

eIF6 enhances OSCC proliferation in vitro and in vivo. (A) Efficiency of eIF6 overexpression and knock-down was assessed by qRT-PCR and Western blotting analysis. (B) Colony formation assay in eIF6 over-expressed HN4 and HN6 cells. (C) Flow cytometry analysis in eIF6 over-expressed HN4 and HN6 cells. (D) CCK8 assay of eIF6 overexpression was investigated. eIF6 greatly promoted cell proliferation. (E-F) eIF6 knockdown resulted in anti-proliferative effect in colony formation and flow cytometry analysis. (G) CCK-8 assays confirmed the anti-proliferative effect of eIF6 in OSCC cell lines. (H-I) eIF6 over-expression promoted tumor growth and depletion of eIF6 inhibited tumor progression in vivo. The tumors dissected

from mice were presented. Tumor weight and tumor volume were demonstrated on the right respectively. *P < 0.05, **P < 0.01, ***P < 0.001.

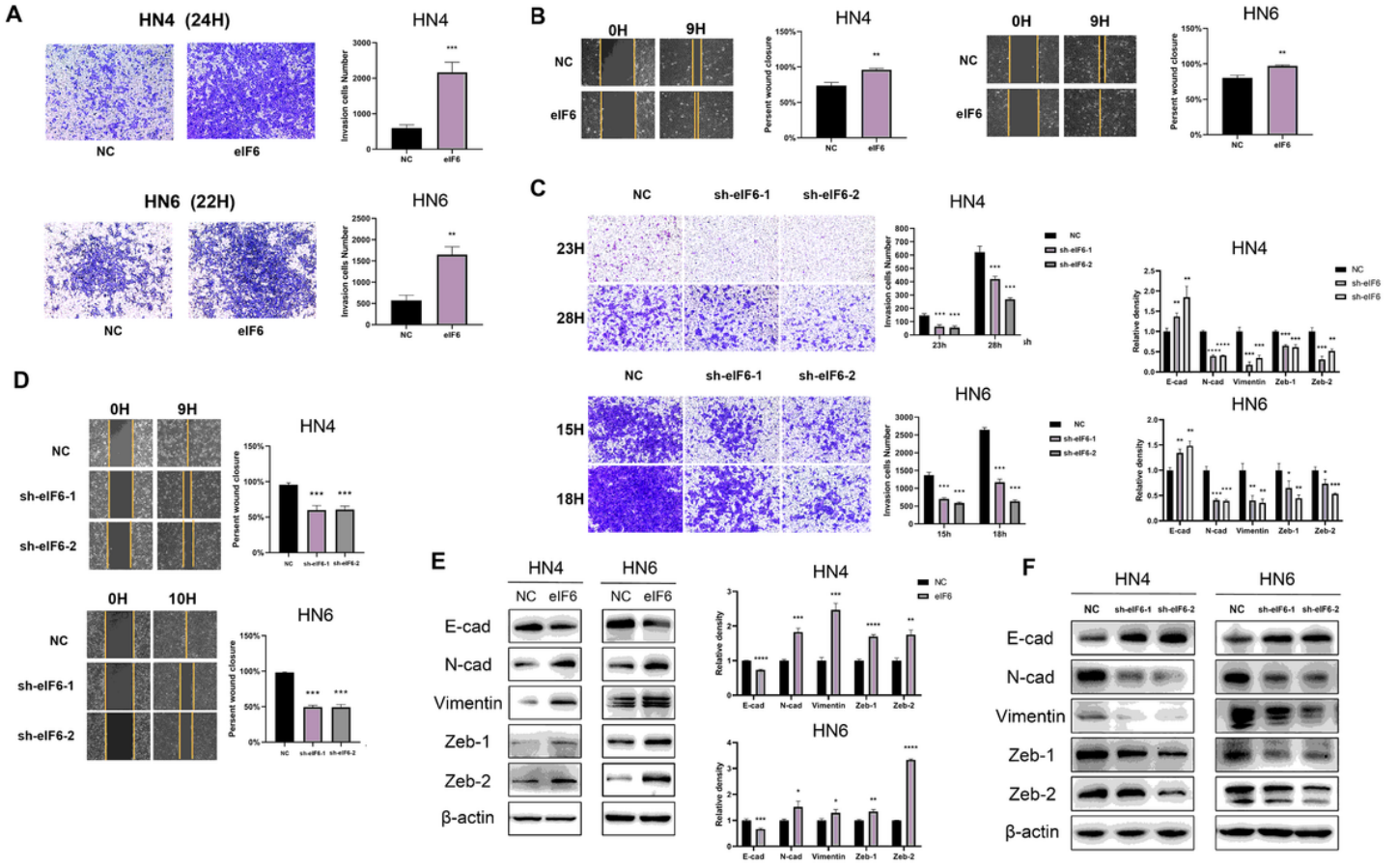

Figure 3

High expression of eIF6 can induce epithelial-mesenchymal transition, while knockdown of eIF6 reversed this process. (A) Transwell experiment was performed in HN4 and HN6 eIF6-transfected or NC-transfected cells (50× magnification). eIF6 enhanced invasive capacity of OSCC cells. (B) The scratch assay was performed in HN4 and HN6 eIF6-transfected cells. (C) Transwell experiment was performed in HN4 and HN6 sh-eIF6-transfected or sh-NC-transfected cells (50× magnification). (D) Wound healing experiment was demonstrated in sh-eIF6-transfected or sh-NC-transfected OSCC cells. (E) The relationship between high expression of eIF6 and EMT-related markers in HN4 and HN6 cells by western blot analysis. (F) Western blot analysis showed the effect of eIF6 knockdown on EMT in HN4 cells. All error bar values represent the SD. *P < 0.05, **P < 0.01, ***P < 0.001.

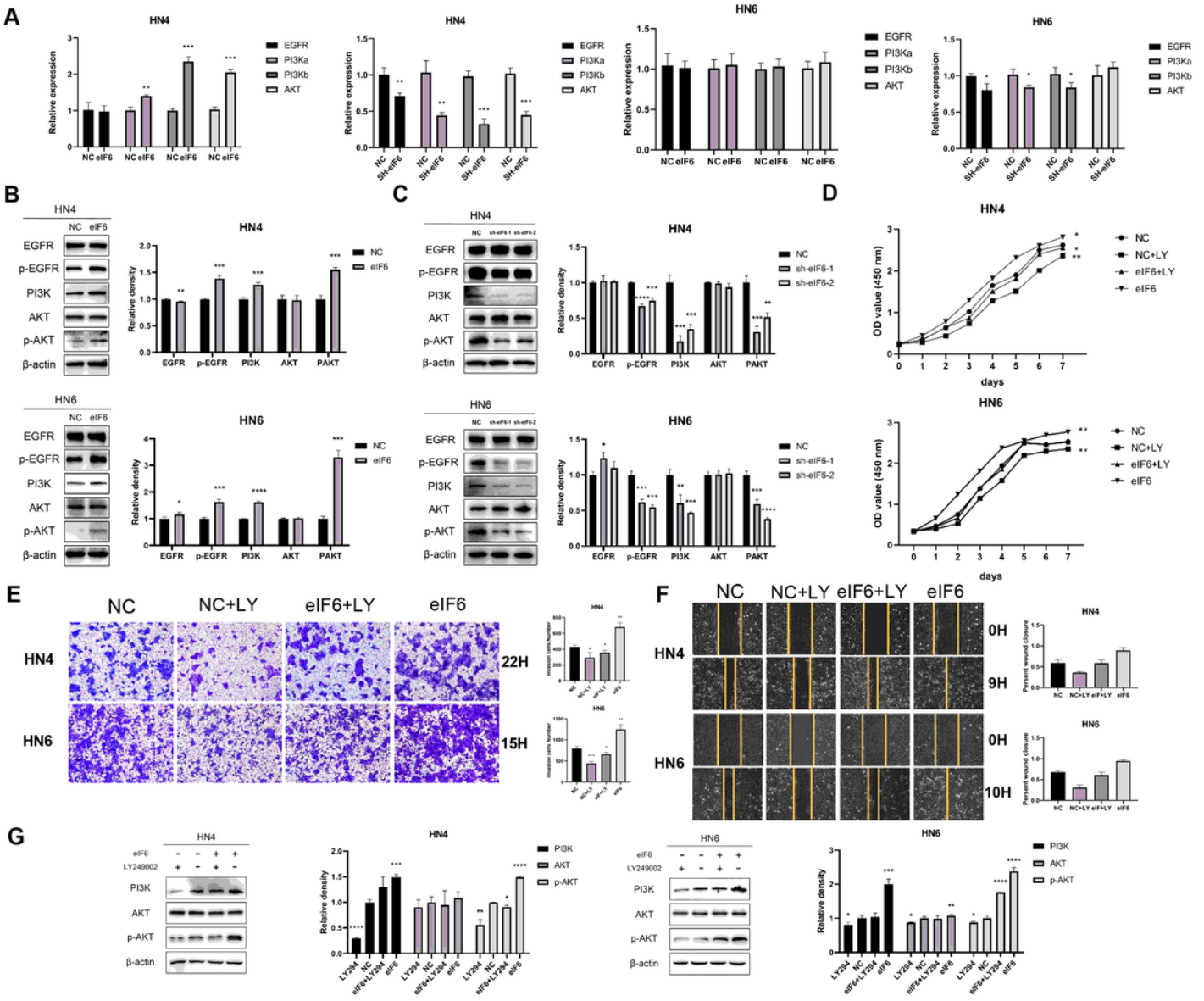

Figure 4

eIF6 effect is related to the AKT signaling pathway. (A) mRNA changes in PIK3CA, PIK3CB, AKT and EGFR upon upregulation or downregulation of eIF6 in OSCC cells. (B) Western blot analysis of EGFR-AKT pathway-related markers after the increase of eIF6 in HN4 and HN6 cells. (C) Inhibition of eIF6 caused a visible reduction in p-EGFR, PI3K, and p-AKT protein expression. (D-F) LY294002 decreased the oncogenic phenotype of eIF6 by depressing proliferative (D), invasive (E) and migrative (F) ability. (G) Western blotting analysis in cells transfected with eIF6 or NC plasmids with or without the treatment of LY294002. All error bar values represent the SD. *P < 0.05, **P < 0.01, ***P < 0.001.

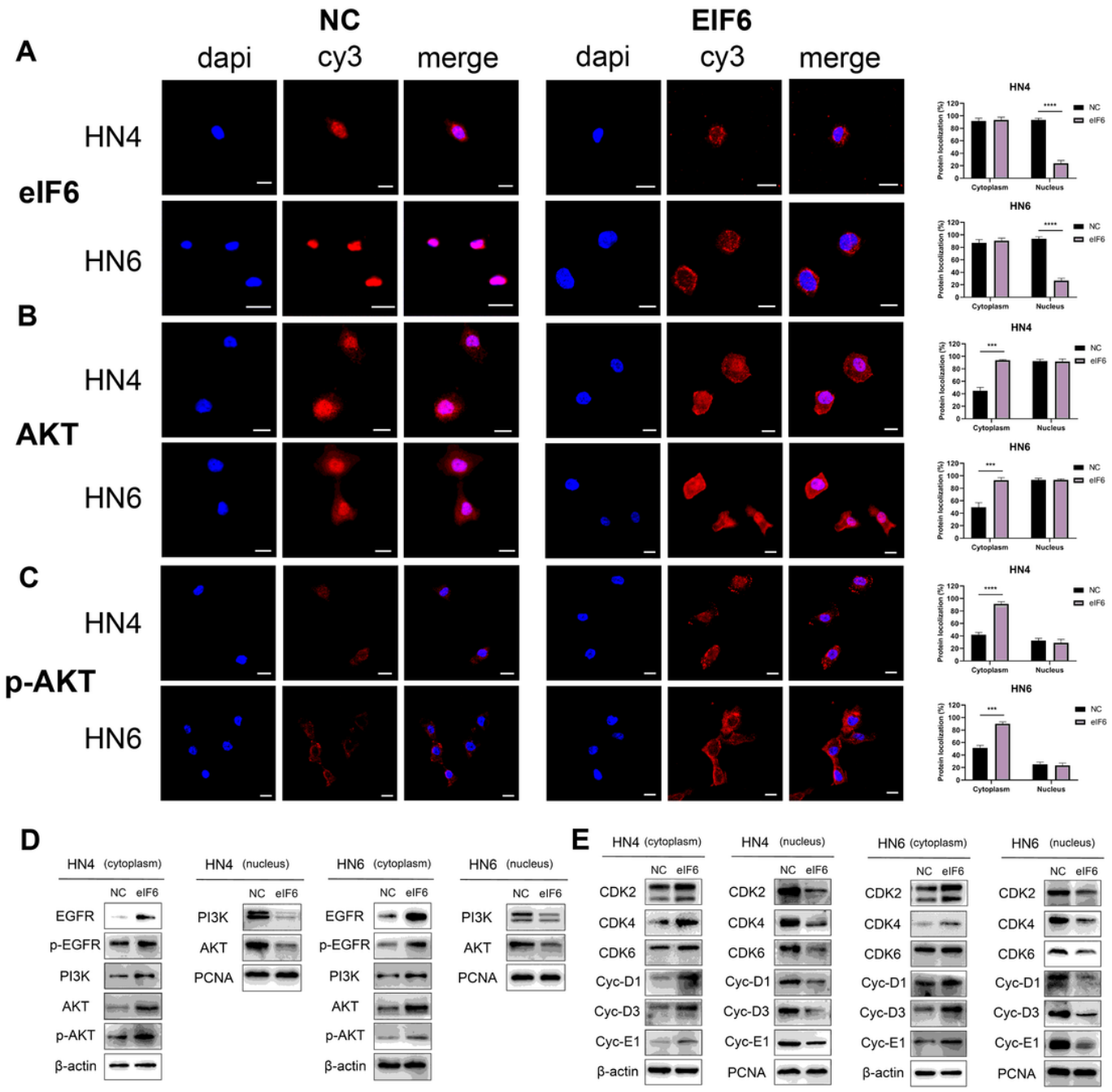

Figure 5

eIF6 participates in the activation of AKT in the cytoplasm. (A) Confocal microscopy showed that eIF6 was mainly expressed in the cytoplasm upon eIF6 amplification compared with control. (eIF6, red; DAPI depicts nuclei, blue). (B-C) Increased immunostaining of AKT (B) and p-AKT (C) in the cytoplasm was shown upon ectopic expression of eIF6. (D) eIF6 augmentation resulted in the upregulation of cytoplasmic expression of eIF6, AKT and p-AKT, while nucleus expression of eIF6, AKT and p-AKT was reduced after transfection. (E) Cell-cycle related proteins were further analyzed in the subcellular fractions. All error bar values represent the SD. Scale bar, 20 μm. *P < 0.05, **P < 0.01, ***P < 0.001.

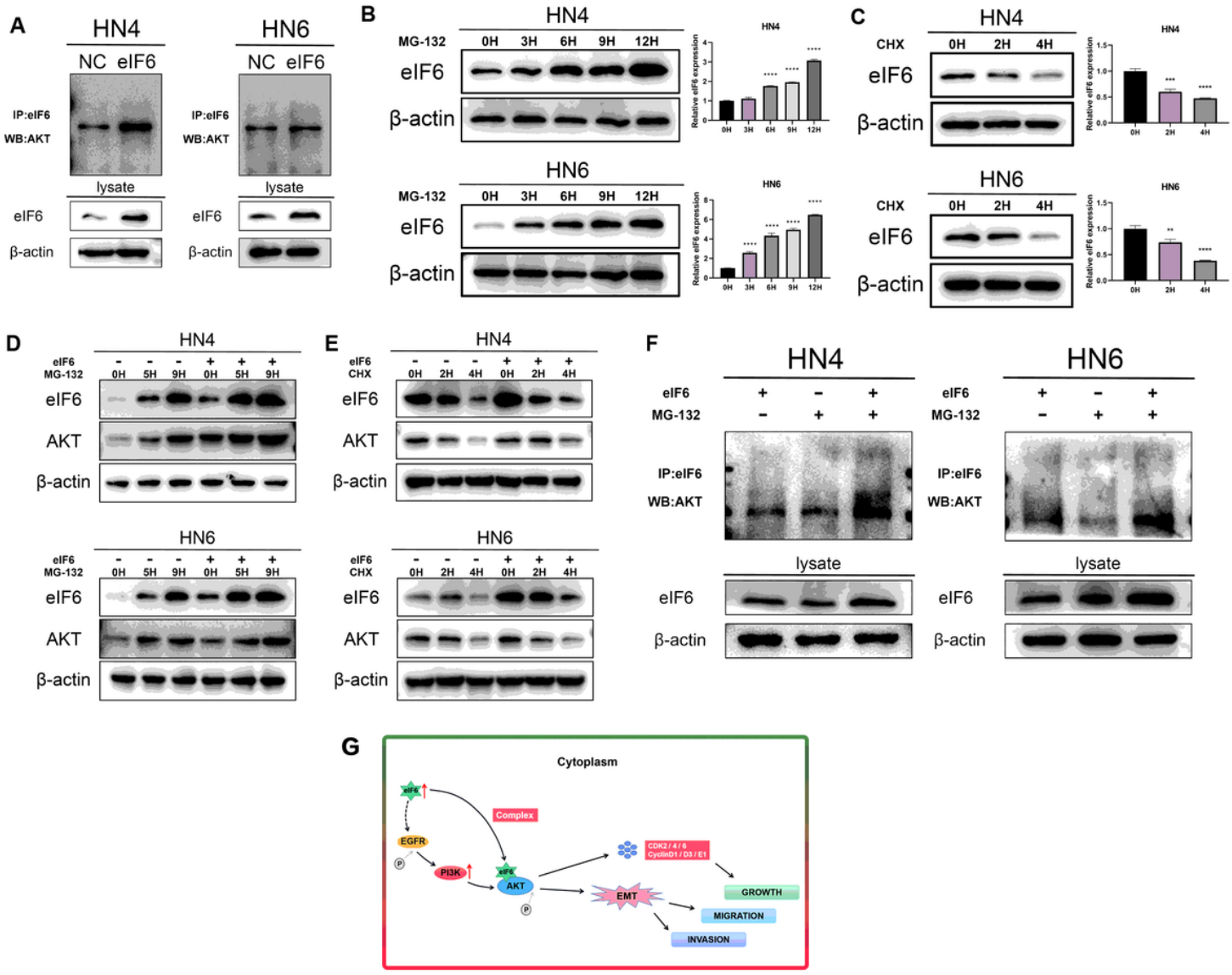

Figure 6

eIF6 physically interacts with AKT. (A) Immunoprecipitation assay between endogenous eIF6 and AKT. (B) The protein levels of eIF6 and AKT were detected in cells treated with MG132 (10 μM). (C) The protein levels of eIF6 and AKT were detected in cells treated with CHX (20 μM). (D) Cells over-expressing eIF6 were treated with or without MG132, and the eIF6 and AKT protein levels were assessed by Western blotting. (E) CHX was utilized in cells transformed with eIF6 or NC plasmids, and the protein expression levels of eIF6 and AKT were displayed. (F) Co-IP experiment showed MG132 promoted the binding extent between eIF6 and AKT. The cells in eIF6 over-expression group were treated with or without MG132. Cell lysates were prepared and subjected to immunoprecipitation with anti-eIF6 antibody. The level of AKT was detected by western blotting analysis. (G) Graphical abstract demonstrated the regulation of eIF6/AKT axis in the cytoplasm.

Supplementary Files

This is a list of supplementary files associated with this preprint. Click to download.

- TableS1.docx